Multiple-temperature kinetic model for continuum and near continuum flows

Kun Xu[a] and Hongwei Liu
Mathematics Department, Hong Kong University of Science and Technology, Clear Water Bay, Kowloon, Hong Kong

Jianzheng Jiang
Institute of Mechanics, Chinese Academy of Sciences, Beijing, China

(Received 16 May 2006; accepted 4 December 2006; published online 11 January 2007)

A gas-kinetic model with multiple translational temperature for the continuum and near continuum flow simulations is proposed. The main purpose for this work is to derive the generalized Navier-Stokes equations with multiple temperature. It is well recognized that for increasingly rarefied flowfields, the predictions from continuum formulation, such as the Navier-Stokes equations lose accuracy. These inaccuracies may be partially due to the single temperature assumption in the standard Navier-Stokes equations. Here, based on an extended Bhatnagar-Gross-Krook (BGK) model with multiple translational temperature, the numerical scheme for its corresponding Navier-Stokes equations is also constructed. In the current approach, the energy exchange between x, y, and z directions is modeled through the particle collision, and individual energy equation in different direction is obtained. The kinetic model, newly constructed is an enlarged system in comparison with Holway's ellipsoid statistical BGK model (ES-BGK). The detailed difference is presented in this paper. In the newly derived "Navier-Stokes" equations from the current model, all viscous terms are replaced by the temperature relaxation terms. The relation between the stress and strain in the standard Navier-Stokes equations is recovered only in the limiting case when the flow is close to the equilibrium, such as small temperature differences in different directions. In order to validate the generalized Navier-Stokes equations, we apply them to the study of Couette and Poiseuille flows with a wide range of Knudsen numbers. In the continuum flow regime, the standard Navier-Stokes solutions are precisely recovered. In the near continuum flow regime, the simulation results are compared with the direct simulation Monte Carlo solutions. The anomalous phenomena in the pressure and temperature distributions from the standard Navier-Stokes equations in the Poiseuille flow case at $\mathrm{Kn}=0.1$ are well resolved by the generalized Navier-Stokes equations. This paper clearly shows that many thermal nonequilibrium phenomena in the near continuum flow regime can be well captured by modifying some assumptions in the standard Navier-Stokes equations. © *2007 American Institute of Physics*. [DOI: 10.1063/1.2429037]

I. INTRODUCTION

The transport phenomena, i.e., mass, heat, and momentum transfer in different flow regime, are of a great scientific and practical interest. The classification of various flow regimes is based on the dimensionless parameter, i.e., the Knudsen number, which is a measure of the degree of rarefaction of the medium. The Knudsen number Kn is defined as the ratio of the mean free path to a characteristic length scale of the system. In the continuum flow regime where $\mathrm{Kn}<0.001$, the Navier-Stokes (NS) equations with linear relations between stress and strain and the Fourier's law for heat conduction are adequate to model the fluid behavior. For flows in the continuum-transition regime ($0.1<\mathrm{Kn}<1$), the Navier-Stokes equations are known to be inadequate. This regime is important for many practical engineering problems, such as the simulation of microscale flows[1] and hypersonic flow around space vehicles in low Earth orbit.[2] Hence, there is a strong desire and requirement for accurate models that give reliable solutions with lower computational costs.

Currently, the direct simulation Monte Carlo (DSMC) method is the most successful technique in the numerical prediction of low density flows.[3] However, in the continuum-transition regime, especially for the microchannel flows, the DSMC suffers from statistical noise in the bulk velocity because of the random molecular motion. When the bulk velocity is much slower than the thermal velocity, many independent samples are needed to eliminate the statistical scattering, as for the microelectromechanical system (MEMS) simulation. In fact, for the nitrogen gas at room temperature, the standard deviation in the molecular speed is about 300 m/s, which would require approximately 9×10^6 independent samples in DSMC to reduce the scatter in the bulk velocity to 0.1 m/s. For MEMS gas flows that operate in the mm/s range, the number of required samples can grow into trillions. Thus, DSMC is impractical in these cases. Alternatively, many macroscopic continuum models have been intensively developed in the literature. These include the

[a]Author to whom correspondence should be addressed. Electronic mail: makxu@ust.hk

Navier-Stokes and the Burnett equations from the Chapman-Enskog expansion, Grad's 13 moment equations, the regularized 13 equations, and many others. In order to validate these continuum models, a few test cases have been used.[4] It seems that none of the models is commonly acceptable for rarefied flow simulations. In addition, in most above models, a single translational temperature is usually assumed. Overall, the small length scales and slow bulk gas velocity combine to make continuum solutions inaccurate, and particle solution time consuming. Besides DSMC and continuum models, many alternative approaches have also been proposed in recent years, such as the empirical slip and viscosity model,[5] the information preservation (IP) method,[6,7] and the lattice Boltzmann method (LBM).[8] However, IP and LBM are mostly used for the isothermal flows. Recently, advances have been made in LBM method to describe nonisothermal behavior,[9] and many successful applications in microflows have been obtained.[10]

Based on a closed solution of the BGK model, a generalization of particle collision time or constitutive relationship has been obtained for nonequilibrium flow.[11,12] The derived extended Navier-Stokes equations from the BGK model with a generalized constitutive relationship, i.e., extended viscosity and heat conduction coefficients to rarefied regime, have been successfully used in the argon and nitrogen shock structures for a wide range of Mach numbers, i.e., $1.2 \leqslant \mathrm{Ma} \leqslant 11$. The current study is to further modify the kinetic BGK model, construct new Navier-Stokes equations with multiple translational temperature, and apply it to capture thermal nonequilibrium phenomena in the near continuum flow regime. The major point we will deliver is that in order to capture thermal nonequilibrium effect, the stress strain relationship in the Navier-Stokes equations has to be replaced by the temperature relaxation terms. In the continuum flow regime, the temperature relaxation goes back automatically to the Navier-Stokes assumption.

In this paper, Sec. II provides details on the construction of the kinetic equation and its generalized Navier-Stokes equations. Section III describes the gas-kinetic scheme to solve the newly constructed Navier-Stokes equations. Section IV concerns the application of the current scheme to flow computation from continuum to the near continuum regime, i.e., $0.001 < \mathrm{Kn} < 0.5$. The numerical solutions from the current model are compared with the exact Navier-Stokes solutions in the continuum flow regime and the DSMC results in the transition flow regime. The final section is the conclusion.

II. MULTIPLE TRANSLATIONAL TEMPERATURE KINETIC MODEL AND ITS GENERALIZED NAVIER-STOKES EQUATIONS

In this section, we first review the BGK equation, construct the multiple-temperature (multi-T) kinetic model for monatomic gas, and derive its macroscopic Navier-Stokes equations for both continuum and near continuum flow simulation.

A. Standard BGK model and Navier-Stokes equations

The Boltzmann equation expresses the behavior of a many-particle kinetic system in terms of the evolution equation for a single-particle gas distribution function. The simplification of the Boltzmann equation given by the BGK model is formulated as[13]

$$\frac{\partial f}{\partial t} + \mathbf{u} \cdot \frac{\partial f}{\partial \mathbf{x}} = \frac{f^{\mathrm{eq}} - f}{\tau}, \tag{1}$$

where f is the number density of molecules at position $\mathbf{x}$ and particle velocity $\mathbf{u}=(u,v,w)$ at time t. The left-hand side of the above equation represents the free streaming of molecules in space, and the right side denotes the collision term. If the distribution function f is known, macroscopic variables, such as mass, momentum, energy, and stress, can be obtained by taking the moments of the gas distribution function. In the BGK model, the collision operator is approximated by a simple relaxation term, where f approaches a local equilibrium given by f^{eq} in a characteristic time scale τ. Traditionally, the equilibrium state is given by a single-temperature Maxwellian,

$$f^{\mathrm{eq}} = \rho\left(\frac{\lambda}{\pi}\right)^{(K+3)/2} e^{-\lambda[(\mathbf{u}-\mathbf{U})^2+\xi^2]},$$

where ρ is the density, $\mathbf{U}$ the macroscopic fluid velocity, and $\lambda = m/2kT$. Here, m is the molecular mass, k is the Boltzmann constant, and T is the temperature. For an equilibrium flow, the internal variable ξ accounts for the rotational and vibrational modes, such as $\xi^2 = \xi_1^2 + \xi_2^2 + \cdots + \xi_K^2$, and the total number of degrees of freedom K is related to the specific heat ratio γ. In the current paper, we only consider monatomic gas with $K=0$. The relation between mass ρ, momentum $\rho\mathbf{U}$, and energy densities ρE with the distribution function f becomes

$$\begin{pmatrix} \rho \\ \rho\mathbf{U} \\ \rho E \end{pmatrix} = \int \psi_\alpha f d\mathbf{u}, \tag{2}$$

where ψ_α is the component of the vector of moments

$$\psi = \left(1, \mathbf{u}, \frac{1}{2}\mathbf{u}^2\right)^T,$$

with $d\mathbf{u} = du\, dv\, dw$ and $\mathbf{u}^2 = u^2 + v^2 + w^2$. Since mass, momentum, and energy are conserved during particle collisions, f and f^{eq} satisfy the conservation constraint

$$\int (f^{\mathrm{eq}} - f)\psi_\alpha d\mathbf{u} = 0, \tag{3}$$

at any point in space and time.

The BGK model was originally proposed to describe the essential physics of molecular interactions with τ chosen as the molecular collision time. Although the BGK model appears to describe only weak departures from local equilibria, it has long been recognized that such an approximation works well beyond its theoretical limits as long as the relaxation time is known for a physical process. Based on the

above BGK model, the Navier-Stokes equations can be derived with the Chapman-Enskog expansion truncated to the first order:

$$f = f^{\mathrm{eq}} + \mathrm{Kn}\, f_1 = f^{\mathrm{eq}} - \tau(\partial f^{\mathrm{eq}}/\partial t + \mathbf{u}\cdot\partial f^{\mathrm{eq}}/\partial \mathbf{x}). \tag{4}$$

For the Burnett and super-Burnett solutions, the above expansion can be naturally extended,[14] such as $f=f^{\mathrm{eq}}+\mathrm{Kn}\, f_1 + \mathrm{Kn}^3 f_3 + \cdots$.

Based on the Chapman-Enskog expansion and the BGK model, in the continuum flow limit the Navier-Stokes equations with the stress and Fourier heat conduction terms can be derived. In this paper, in order to make the expression clear, the derived macroscopic governing equations from kinetic model in one-dimensional (1-D) space is presented, but the numerical scheme presented is solving the corresponding multidimensional flow equations. The Navier-Stokes equations derived from the single-temperature BGK model for a monatomic gas in the 1-D case can be written as

$$\begin{pmatrix} \rho \\ \rho U \\ \rho E \end{pmatrix}_t + \begin{pmatrix} \rho U \\ \rho U^2 + p \\ (\rho E + p)U \end{pmatrix}_x = \begin{pmatrix} 0 \\ \frac{4}{3}\mu U_x \\ \frac{5}{2}\mu R T_x + \frac{4}{3}\mu U U_x \end{pmatrix}_x, \tag{5}$$

where $p=\rho RT$ is the pressure and $\mu=\tau p$ is the dynamical viscosity coefficient. With the relation $\lambda=m/2kT=1/2RT$ and $C_p=5k/2m=5R/2$ for a monatomic gas, the heat conduction coefficient in the above equations becomes $\kappa=5k\mu/2m$, and the Prandtl number becomes fixed with the value $\mathrm{Pr}=\mu C_p/\kappa=1$. This is a well known result for the BGK model.

B. Multiple-temperature gas-kinetic model and its corresponding Navier-Stokes equations

Traditionally, the BGK model is considered suitable only for isothermal rarefied gas flow. It does not provide reliable results for nonisothermal flows because it gives incorrect Prandtl number. The disagreement between an exact solution based on the Boltzmann equation and that obtained from the BGK model reaches 30% near the hydrodynamic flow regime. In order to get the correct Prandtl number, many modification of the BGK model have been proposed. One is the ellipsoid-statistical BGK (ES-BGK) model of Holway,[15] and the other is the S-model of Shakhov.[16] In the ES-BGK model, the "temperature" becomes a tensor and it is related to the Prandtl number. In the S-model, a heat flux term is added in the equilibrium state. In our early BGK scheme for solving the compressible Navier-Stokes equations in the continuum flow computation,[17] the correct Prandtl number is achieved through the modification of heat flux across a cell interface in a finite volume scheme. In the following, we are going to propose a multi-T model. The purpose of constructing such a model is not for the Prandtl number correction, but for the derivation of the generalized Navier-Stokes equations with the inclusion of multiple translational temperature for the near continuum flow, where the traditional NS equations are not adequate.

Since this paper concerns the mainly two-dimensional (2-D) flow simulations, a 2-D multi-T kinetic model will be presented. The generalized BGK model has the same form as the original one,

$$\frac{\partial f}{\partial t} + u\frac{\partial f}{\partial x} + v\frac{\partial f}{\partial y} = \frac{g-f}{\tau}, \tag{6}$$

but the equilibrium state has multiple temperatures,

$$g = \rho\left(\frac{\lambda_x}{\pi}\right)^{1/2}\left(\frac{\lambda_y}{\pi}\right)^{1/2}\left(\frac{\lambda_z}{\pi}\right)^{1/2} \times \exp[-\lambda_x(u-U)^2 - \lambda_y(v-V)^2 - \lambda_z w^2]. \tag{7}$$

Here, $\lambda_x=m/(2kT_x)$, $\lambda_y=m/(2kT_y)$, and $\lambda_z=m/(2kT_z)$ are related to the translational temperature T_x, T_y, and T_z in the x, y, and z directions. In order to determine all unknowns in the corresponding macroscopic variables, such as ρ, U, V, T_x, T_y, and T_z, we propose the following moments for the collision term of the BGK model:

$$\int \phi\left(\frac{\partial f}{\partial t} + u\frac{\partial f}{\partial x} + v\frac{\partial f}{\partial y}\right) du\, dv\, dw = \int \phi\frac{g-f}{\tau} du dv dw = \begin{pmatrix} 0 \\ 0 \\ 0 \\ 0 \\ (\rho E_x^{\mathrm{eq}} - \rho E_x)/\tau \\ (\rho E_y^{\mathrm{eq}} - \rho E_y)/\tau \end{pmatrix}, \tag{8}$$

where

$$\phi = \left[1, u, v, \frac{1}{2}(u^2+v^2+w^2), \frac{1}{2}u^2, \frac{1}{2}v^2\right]^T.$$

The first four moments on the right-hand side of Eq. (8) are the conservative moments of the mass, momentum, and total energy, which have zero values due to the conservation during particle collision. The last two moments are the models proposed to simulate the energy exchange in different directions. The equilibrium energies ρE_x^{eq} and ρE_y^{eq} in Eq. (8) have the forms

$$\rho E_x^{\mathrm{eq}} = \frac{1}{2}\rho U^2 + \frac{\rho}{4\lambda^{\mathrm{eq}}},$$

and

$$\rho E_y^{\mathrm{eq}} = \frac{1}{2}\rho V^2 + \frac{\rho}{4\lambda^{\mathrm{eq}}},$$

which are constructed based on the assumption that the system will approach to an equilibrium state with equal temperature. The common equilibrium temperature, i.e., λ^{eq}, in all directions is determined by equally distributing thermal energy in all degrees of freedom,

$$\rho\frac{3}{4\lambda^{\mathrm{eq}}} = \rho E - \frac{1}{2}\rho(U^2 + V^2),$$

where ρE is the total energy, i.e.,

$$\rho E = \int \frac{1}{2}(u^2 + v^2 + w^2) f du\, dv\, dw$$

$$= \int \frac{1}{2}(u^2 + v^2 + w^2) g du\, dv\, dw.$$

The tendency for the gas distribution function to approach to a common Maxwellian determined by $(\rho, U, V, \lambda^{\mathrm{eq}})$ means that the H-theorem for the system (6) and (8) is satisfied. Note that the last two moments on the right-hand side of Eq. (8) cannot be derived directly from the BGK equation (6) itself. It is a model we construct. The basic consideration is that there needs particle collision to exchange energy in different directions. The direct moments $(\frac{1}{2}u^2, \frac{1}{2}v^2)$ to the BGK equation (6) with the multiple-temperature equilibrium state g in Eq. (7) will give

$$\left[\rho\left(\frac{1}{2}U^2 + \frac{1}{4\lambda_x}\right) - \rho E_x\right]/\tau$$

and

$$\left[\rho\left(\frac{1}{2}V^2 + \frac{1}{4\lambda_y}\right) - \rho E_y\right]/\tau,$$

for the two terms on the right-hand side of Eq. (8), which are not adequate to close the system due to the three unknowns $(\lambda_x, \lambda_y, \lambda_z)$ instead of one. In other words, the multiple-temperature equilibrium state in Eq. (6) includes two more unknowns, such as λ_y and λ_z. In order to close the system to have a unique solution, we have to introduce two more equations or constraints, which are the last two moments in (8), where λ^{eq} can be explicitly determined through the total thermal energy in the system. Thus, the above multi-T BGK model is an extension of the original BGK model and the nonconservative moments are modeled instead of directly derived from the BGK collision term. In the above model, the thermal equilibrium among x, y, and z directions will be achieved through the particle collisions, and there will be a time delay to achieve such a temperature equilibrium. In the standard Navier-Stokes equations, it is assumed that the same equilibrium temperature in different directions is obtained instantaneously. As shown in the following, the Navier-Stokes assumption between the stress and the velocity gradient is valid mainly in the continuum flow limit. The real viscosity terms in the NS equations will be replaced by the temperature relaxation term. The Chapman-Enskog expansion of the multi-T kinetic model will present generalized NS equations, and they go back to the traditional ones when the temperature differences among T_x, T_y, and T_z are small. In order to make the presentation clear, even for the above 2-D kinetic model, in the following, we are going to apply it to the one-dimensional flow and derive the corresponding macroscopic governing equations. However, in terms of the numerical scheme presented in section III, the 2-D generalized Navier-Stokes equations will be solved.

Based on the multi-T kinetic model, in the 1-D case the equilibrium state can be written as

$$g = \rho\left(\frac{\lambda^{\parallel}}{\pi}\right)^{1/2}\left(\frac{\lambda^{\perp}}{\pi}\right)\exp[-\lambda^{\parallel}(u-U)^2 - \lambda^{\perp}\xi^2],$$

where ξ represents the particle random motion in y, and z directions, i.e., $\xi^2 = v^2 + w^2$, and the $\lambda^{\parallel} = 1/2RT^{\parallel}$ and $\lambda^{\perp} = 1/2RT^{\perp}$ represent the x-direction temperature $T^{\parallel}$ and the temperature $T^{\perp}$ in other directions. For the equilibrium flow with $T^{\parallel} = T^{\perp}$, the inviscid governing equations, i.e., the Euler equations, can be obtained from Eq. (6),

$$\begin{pmatrix} \rho \\ \rho U \\ \frac{1}{2}\rho(U^2 + RT^{\parallel} + 2RT^{\perp}) \end{pmatrix}_t + \begin{pmatrix} \rho U \\ \rho U^2 + \rho RT^{\parallel} \\ \frac{1}{2}\rho U(U^2 + 3RT^{\parallel} + 2RT^{\perp}) \end{pmatrix}_x = \begin{pmatrix} 0 \\ 0 \\ 0 \end{pmatrix}. \tag{9}$$

Even though $T^{\parallel} = T^{\perp}$ in the above equilibrium flow, in order to distinguish the different contribution to the energy and corresponding fluxes from the random motion in different directions, the distinguishable temperatures $T^{\parallel}$ and $T^{\perp}$ are still used. By using the first-order Chapman-Enskog expansion, the following dissipative governing equations from the kinetic model (6) can be obtained:

$$\begin{pmatrix} \rho \\ \rho U \\ \frac{1}{2}\rho(U^2+RT^{\parallel}+2RT^{\perp}) \\ \rho RT^{\perp} \end{pmatrix}_t + \begin{pmatrix} \rho U \\ \rho U^2+\rho RT^{\parallel} \\ \frac{1}{2}\rho U(U^2+3RT^{\parallel}+2RT^{\perp}) \\ \rho URT^{\perp} \end{pmatrix}_x = \begin{pmatrix} 0 \\ -\frac{2}{3}\rho R(T^{\parallel}-T^{\perp}) \\ \frac{3}{2}\tau\rho R^2T^{\parallel}(T^{\parallel})_x+\tau\rho R^2T^{\parallel}(T^{\perp})_x-\frac{2}{3}\rho RU(T^{\parallel}-T^{\perp}) \\ \tau\rho R^2T^{\parallel}(T^{\perp})_x+\frac{1}{3}\rho RU(T^{\parallel}-T^{\perp}) \end{pmatrix}_x + \begin{pmatrix} 0 \\ 0 \\ 0 \\ \frac{\rho}{3\tau}R(T^{\parallel}-T^{\perp}) \end{pmatrix}. \tag{10}$$

The above equations are different from the standard Navier-Stokes equations (5) derived from the single temperature BGK model. Instead of the viscous flux $(4/3)\mu U_x$ in (5), the current model replaces it by the temperature relaxation term, i.e., $-(2/3)\rho R(T^{\parallel}-T^{\perp})$. Near the thermal equilibrium limit, i.e., $T^{\parallel}\simeq T^{\perp}\simeq T^{\mathrm{eq}}$, the temperature difference becomes

$$T^{\parallel}-T^{\perp}=-2\tau T^{\mathrm{eq}}U_x.$$

Therefore, the relaxation term in the momentum equation goes to

$$-\tfrac{2}{3}\rho R(T^{\parallel}-T^{\perp})=\tfrac{4}{3}\tau\rho RT^{\mathrm{eq}}U_x,$$

which exactly recovers the viscous term in the standard Navier-Stokes equations. In addition, the total energy dissipative flux becomes

$$\tfrac{4}{3}\tau\rho RT^{\mathrm{eq}}UU_x+\tfrac{5}{2}\tau\rho R^2T^{\mathrm{eq}}T_x^{\mathrm{eq}},$$

where the pressure becomes $p=\rho RT^{\mathrm{eq}}$. Thus, in the thermal equilibrium limit, the standard Navier-Stokes equations are obtained, and the thermal energy equation in (10) becomes a dependent equation that can be derived from the total energy and momentum equations. Hence, the multi-T kinetic model corresponds to an enlarged Navier-Stokes equations, and this system shrinks to the standard NS equations in the continuum limit. As presented in the numerical experiments, in the continuum flow regime, i.e., $\mathrm{Kn}\leqslant 0.01$, the solution from the enlarged system does recover the exact Navier-Stokes solution. The nonequilibrium thermal effect only takes places when Kn becomes large, such as in the near continuum flow regime. In order to validate the generalized Navier-Stokes equations, instead of solving Eq. (10) directly, we are going to solve numerically the kinetic model (6) to the Navier-Stokes order using BGK-NS scheme, which is presented in Sec. III.

From the above relaxation model, we can realize that the viscous term approximation in the Navier-Stokes equations is not an intrinsic property of a gas, but rather, an approximation designed to simulate the effect of thermal relaxation when the governing equations are cast in terms of a single temperature. This approximation is based on the assumption that the time scale of the macroscopic gas motion is much larger than the relaxation time for the thermal energy equilibrium. This local thermodynamic equilibrium assumption is a good approximation only for low Knudsen number flows. When the characteristic time for temperature relaxation is comparable to the characteristic flow time scale in the near continuum flow regime, the relaxation effect has to be considered.

C. Comparison between multi-T kinetic model and ES-BGK model

Based on the first-order Chapman-Enskog expansion, the original BGK model gives the Navier-Stokes equations with unit Prandtl number. In order to obtain a proper Prandtl number for a realistic flow, Holway suggested the ES-BGK model,[15] where the Maxwellian distribution in the BGK model is replaced by an anisotropic Gaussian so that the collision term reads

$$Q=(g_h-f)/\tau,$$

where g_h denotes the anisotropic Gaussian,

$$g_h=\frac{\rho}{\sqrt{2\pi\lambda_{ij}}}\exp\left[-\frac{1}{2}\lambda_{ij}^{-1}C_iC_j\right],$$

and the matrix λ_{ij} is given by

$$\lambda_{ij}=RT\delta_{ij}+\left(1-\frac{1}{\mathrm{Pr}}\right)\frac{p_{ij}}{\rho}.$$

Here, λ_{ij}^{-1} denotes the inverse matrix. Same as the BGK model, the ES-BGK assumes that the collision frequency is independent of the microscopic velocity. An entropy condition for ES-BGK has been recently proved by Andries *et al.*[18] The above ES-BGK model is different from the kinetic model we proposed in the last subsection. For example, for the 1-D flow, the equilibrium state from the above ES-BGK model has the form,

$$g_h = \frac{\rho}{(2\pi)^{3/2}} \frac{1}{\lambda_{11}^{1/2}\lambda_{22}} \exp\left[-\frac{(u-U)^2}{2\lambda_{11}} - \frac{(v^2+w^2)}{2\lambda_{22}} \right],$$

where

$$\lambda_{11} = \left(1 - \frac{\Pr - 1}{\Pr}\right) RT + \frac{1}{\rho}\frac{\Pr - 1}{\Pr} \int (u-U)^2 f du\, dv\, dw,$$

and

$$\lambda_{22} = \left(1 + \frac{1}{2}\frac{\Pr - 1}{\Pr}\right) RT - \frac{1}{2\rho}\frac{\Pr - 1}{\Pr} \times \int (u-U)^2 f du\, dv\, dw,$$

are determined from the moments of f with a local temperature T. As shown above, the Prandtl number is involved in the determination of λ_{11} and λ_{22}. Physically, λ_{11} and λ_{22} in the ES-BGK model are only components of a matrix which have no direct meaning to the temperature. The real temperature in ES-BGK is T, and λ_{ij} is used mainly for the recovery of correct Pr number by modifying the viscosity coefficient to $\mu = \tau\rho RT \Pr$. In addition, the evaluation of λ_{ij} is through the moments of f, which is different from our model, where independent governing equations for the thermal energy (or temperature) in different directions are proposed. In our multi-T model, the modification of Pr number is not our concern. For a flow with Pr=1, the ES-BGK model will go back to the standard BGK model with a single "temperature," i.e., $\lambda_{11}=\lambda_{22}=\lambda_{33}$. However, the multiple temperatures still exist at Pr=1 in our proposed model. Using the Chapman-Enskog expansion, to the first order of Kn, the standard Navier-Stokes equations will be derived from the ES-BGK model. As presented in the last subsection, our multi-T model has an enlarged Navier-Stokes system (10).

III. FINITE VOLUME BGK SCHEME FOR THE GENERALIZED NAVIER-STOKES EQUATIONS

The macroscopic governing equations derived from the new kinetic model in the previous section will be solved using the gas-kinetic BGK scheme.[17] It is a conservative multiscale finite volume method, in which the update of the macroscopic flow variables is through the numerical fluxes at cell interfaces which are evaluated based on the time-dependent gas distribution function. Since we are going to develop a directional splitting method to solve Eq. (6), the kinetic model in x direction can be written as

$$f_t + uf_x = (g - f)/\tau,$$

where g is the multiple-temperature equilibrium state (7). Taking moments ϕ to the above equations in a control volume $x \in [x_{j-1/2}, x_{j+1/2}]$ and time interval $t \in [t^n, t^{n+1}]$, the update of the macroscopic flow variables, i.e., $\mathbf{W} = (\rho, \rho U, \rho V, \rho E, \rho E_x, \rho E_y)^T$ inside each numerical cell $[x_{j-1/2}, x_{j+1/2}]$ from time step t^n to t^{n+1}, becomes

$$\mathbf{W}_j^{n+1} = \mathbf{W}_j^n + \frac{1}{\Delta x}\int_{t^n}^{t^{n+1}} (\mathbf{F}_{j-1/2}(t) - \mathbf{F}_{j+1/2}(t))dt + \mathbf{S}_j^n \Delta t, \tag{11}$$

where $\mathbf{F}_{j+1/2}$ are the corresponding fluxes at a cell interface, which are evaluated based on the gas distribution function $f_{j+1/2}$ there,

$$\mathbf{F} = \int u\phi f_{j+1/2} du\, dv\, dw.$$

The source term is due to the moments of the collision term in Eq. (8), which has the form

$$\mathbf{S} = [0,0,0,0,(\rho E_x^{\mathrm{eq}} - \rho E_x)/\tau, (\rho E_y^{\mathrm{eq}} - \rho E_y)/\tau]^T.$$

For the current multi-T model, the evaluation of the gas distribution function f at a cell interface is similar to the BGK-NS method in Ref. 17, where the only difference between them is that three temperatures T_x, T_y, and T_z have to be accounted for. The following is about the calculation of the gas distribution function $f_{j+1/2}$ based on the multi-T model (6).

Based on the multi-T kinetic model, up to the 1st-order expansion to the Navier-Stokes order, we have the following gas distribution:

$$f(x_{j+1/2}, t, u, v, w) = g - \tau(\partial g/\partial t + u\partial g/\partial x) + t\frac{\partial g}{\partial t}, \tag{12}$$

where $-\tau(g_t + ug_x)$ is the Chapman-Enskog expansion and tg_t is the time evolution part.[14] The relation between τ and μ is $\tau = \mu/p$, where μ is the dynamical viscosity coefficient and p is the pressure. For a two-dimensional gas flow, the equilibrium gas distribution function g has the form

$$g = \rho\left(\frac{\lambda_x}{\pi}\right)^{1/2} \exp[-\lambda_x(u-U)^2]\left(\frac{\lambda_y}{\pi}\right)^{1/2} \times \exp[-\lambda_y(v-V)^2]\left(\frac{\lambda_z}{\pi}\right)^{1/2} \exp(-\lambda_z w^2). \tag{13}$$

The connection between macroscopic variables and the distribution function is

$$\mathbf{W} = (\rho, \rho U, \rho V, \rho E, \rho E_x, \rho E_y)^T = \int \phi g du\, dv\, dw.$$

Thus, from the reconstructed initial data $\mathbf{W}(x_{j+1/2}, t^n)$ at the beginning of each time step, the equilibrium state g in Eq. (12) can be uniquely determined at a cell interface. Then, from the spatial derivative $\partial\mathbf{W}/\partial x$ there, we can evaluate $\partial g/\partial x$ in Eq. (12) as the following. Based on the Taylor expansion, the expansion $\partial g/\partial x$ can be expressed as

$$\frac{\partial g}{\partial x} = g\left[\frac{1}{\rho}\frac{\partial \rho}{\partial x} + \frac{1}{2\lambda_x}\frac{\partial \lambda_x}{\partial x} - \frac{\partial}{\partial x}(\lambda_x U^2 + \lambda_y V^2) + \frac{1}{2\lambda_y}\frac{\partial \lambda_y}{\partial x} + \frac{1}{2\lambda_z}\frac{\partial \lambda_z}{\partial x} + 2\frac{\partial(\lambda_x U)}{\partial x}u + 2\frac{\partial(\lambda_y V)}{\partial x}v - \frac{\partial \lambda_x}{\partial x}u^2 - \frac{\partial \lambda_y}{\partial x}v^2 - \frac{\partial \lambda_z}{\partial x}w^2\right] = g[a_1 + a_2 u + a_3 v + a_4 u^2 + a_5 v^2 + a_6 w^2] = ga, \quad (14)$$

where

$$a = a_1 + a_2 u + a_3 v + a_4 u^2 + a_5 v^2 + a_6 w^2.$$

All coefficients in a can be determined from

$$\frac{\partial}{\partial x}\mathbf{W} = \int \phi a g du\, dv\, dw.$$

Since

$$\lambda_x = \rho/[4(\rho E_x - 0.5\rho U^2)],$$

we have

$$\frac{\partial \lambda_x}{\partial x} = -\frac{4\lambda_x^2}{\rho}\left[\frac{\partial(\rho E_x)}{\partial x} - \frac{1}{2}\frac{\partial(\rho U^2)}{\partial x}\right] + \frac{\lambda_x}{\rho}\frac{\partial \rho}{\partial x} = -a_4,$$

$$\frac{\partial \lambda_y}{\partial x} = -\frac{4\lambda_y^2}{\rho}\left[\frac{\partial(\rho E_y)}{\partial x} - \frac{1}{2}\frac{\partial(\rho V^2)}{\partial x}\right] + \frac{\lambda_y}{\rho}\frac{\partial \rho}{\partial x} = -a_5,$$

$$\frac{\partial \lambda_z}{\partial x} = -\frac{4\lambda_z^2}{\rho}\left[\frac{\partial(\rho E - \rho E_x - \rho E_y)}{\partial x}\right] + \frac{\lambda_z}{\rho}\frac{\partial \rho}{\partial x} = -a_6.$$

Let us define

$$\mathcal{A} = \frac{1}{\rho}\left[\frac{\partial(\rho U)}{\partial x} - U\frac{\partial \rho}{\partial x}\right],$$

and

$$\mathcal{B} = \frac{1}{\rho}\left[\frac{\partial(\rho V)}{\partial x} - V\frac{\partial \rho}{\partial x}\right],$$

then,

$$a_3 = -2a_5 V + 2\lambda_y \mathcal{B},$$

$$a_2 = -2a_4 U + 2\lambda_x \mathcal{A},$$

and

$$a_1 = \frac{1}{\rho}\frac{\partial \rho}{\partial x} - a_2 U - a_3 V - a_4\left(U^2 + \frac{1}{2\lambda_x}\right) - a_5\left(V^2 + \frac{1}{2\lambda_y}\right) - a_6\frac{1}{2\lambda_z}.$$

After determining $\partial g/\partial x = ga$ in Eq. (12), the term $\partial g/\partial t = gA$ with

$$A = [A_1 + A_2 u + A_3 v + A_4 u^2 + A_5 v^2 + A_6 w^2],$$

can be obtained by requiring the nonequilibrium part in the Chapman-Enskog expansion vanishing to the moments ϕ,

$$\int \phi(au + A)g du\, dv\, dw = 0,$$

where the six unknowns in A can be uniquely obtained from the above six equations. The procedure to get A is similar to obtaining a. Therefore, the gas distribution function at the cell interface (12) is totally determined, which can be used to evaluate the fluxes.

After the determination of f at a cell interface, we can explicitly evaluate the heat flux there as well. In order to simulate the flow with any realistic Prandtl number, a modification of the heat flux in the energy transport, such as that used in Ref. 17, is also implemented in the present study. Therefore, the current model can simulate flow with any Prandtl number. It needs to be emphasized again that the kinetic scheme presented in this section is targeting to solve the generalized multiple-temperature Navier-Stokes equations, which can be derived from the multi-T kinetic model.

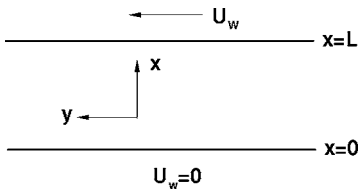

FIG. 1. Couette flow.

IV. NUMERICAL EXPERIMENTS

A. Shear-driven Couette flows

Shear-driven Couette flows are encountered in micromotors, comb mechanisms, and microbearings. In the simplest case, the Couette flow can be used as a prototype flow to model such flows driven by a moving plate. Since the Couette flow is shear driven, the pressure does not change in the streamwise direction. Hence, the compressibility effects become important for large temperature fluctuations or at high speeds. In this section, we simulate the Couette flows in both continuum and near continuum flow regime.

This is a gas flow problem between two infinite parallel plates, separated by a distance L. The schematic structure is shown in Fig. 1. In our computation, the most cases we study are the hard-sphere (HS) molecule and the working gas is argon. The specific heat ratio is $\gamma = 5/3$ with molecular mass $m = 6.63 \times 10^{-26}$ kg. The viscosity coefficient for HS is $\mu = 2.117 \times 10^{-5}\sqrt{(T/273)}$ N s/m^2. The mean free path is defined as

$$l_0 = \frac{16}{5}\left(\frac{1}{2\pi RT}\right)^{1/2}\frac{\mu}{\rho_0},$$

where R is the gas constant, and T and ρ are temperature and density, respectively. In most calculations, both surfaces

maintain 273 K and the Maxwell diffusive kinetic reflection boundary condition[17] are used. The density ρ_0 has a value corresponding to the pressure of 1 atm (or 101 325 Pa) at $T=273$ K. The Knudsen number is defined as $\mathrm{Kn}=l_0/L$, which increases as the length L decreases. In all computations, we use 50 cells in the one-dimensional computational domain.

In order to validate the generalized Navier-Stokes equations in the continuum flow limit, we first apply them to the case, where the exact Navier-Stokes solutions are available. Under the conditions of $\mu \sim T^{\omega}$ with $\omega=1$ and of adiabatic lower wall condition, there is an analytic solution in the compressible case,[19]

$$\frac{\tau_w y}{\mu_\infty U_w} = \frac{U}{U_w} + \mathrm{Pr}\frac{\gamma-1}{2}\mathrm{Ma}_\infty^2\left[\frac{U}{U_w} - \frac{1}{3}\left(\frac{U}{U_w}\right)^3\right],$$

where U_w is the horizontal velocity of the upper wall and Ma_∞ is the corresponding Mach number. In order to test the multi-T BGK scheme, we set up the upper wall with a speed of Ma=3 and lower adiabatic wall with velocity zero, and a Prandtl number Pr=2/3. The viscosity coefficient is set to be $\mu=2.117\times10^{-5}(T/273)$ N s/m^2. The velocity and temperature profiles in the channel are shown in Fig. 2, where the circles are the exact NS solutions and the solid lines are from the current multi-T scheme. In the current case, the Kn number has a value Kn=0.001, which well belongs to the NS flow regime. It is hard to distinguish the three temperatures in the x, y, and z directions in Fig. 2.

In the following, we simulate the Couette flow cases for the hard-sphere (HS) molecules with fixed upper wall velocity 300 m/s. The use of this wall velocity is from the consideration of two aspects. One is the easy solution from the DSMC simulation and the other is the temperature deviation due to large shear. The Prandtl number used is Pr=0.68, which is consistent with the Prandtl number in the DSMC method for the HS model. The Knudsen numbers simulated are Kn=0.01, 0.1, and 0.5. Figure 3 shows the velocity and temperature profiles across the channel at Kn=0.01, where the solid lines are the current multi-T model results and circles are the DSMC solutions. Note three temperatures are plotted for both DSMC and multi-T solutions, even though they are indistinguishable. At this Knudsen number, the separation between the temperature is too small to be seen. As the Knudsen number increases to 0.1, the three temperatures can be clearly observed in Fig. 4, where the magnitudes of the temperature are distributed from the highest T_y, to T_z, and to the lowest T_x. At Kn=0.1, both velocity and temperature from multi-T model have a fair agreement with the DSMC results. As the Kn increases to 0.5, the deviation between different temperature becomes more obvious. Figure 5 shows the velocity and temperature distributions. In this case, the slip velocity due to the kinetic diffusive boundary condition becomes large, and both velocity and temperature distributions come flat in comparison with small Knudsen number results. The temperature in the y direction (same direction as the flow velocity) is higher than those in other two directions. Even though there are deviations close to the boundary in the temperature distributions, the overall match between

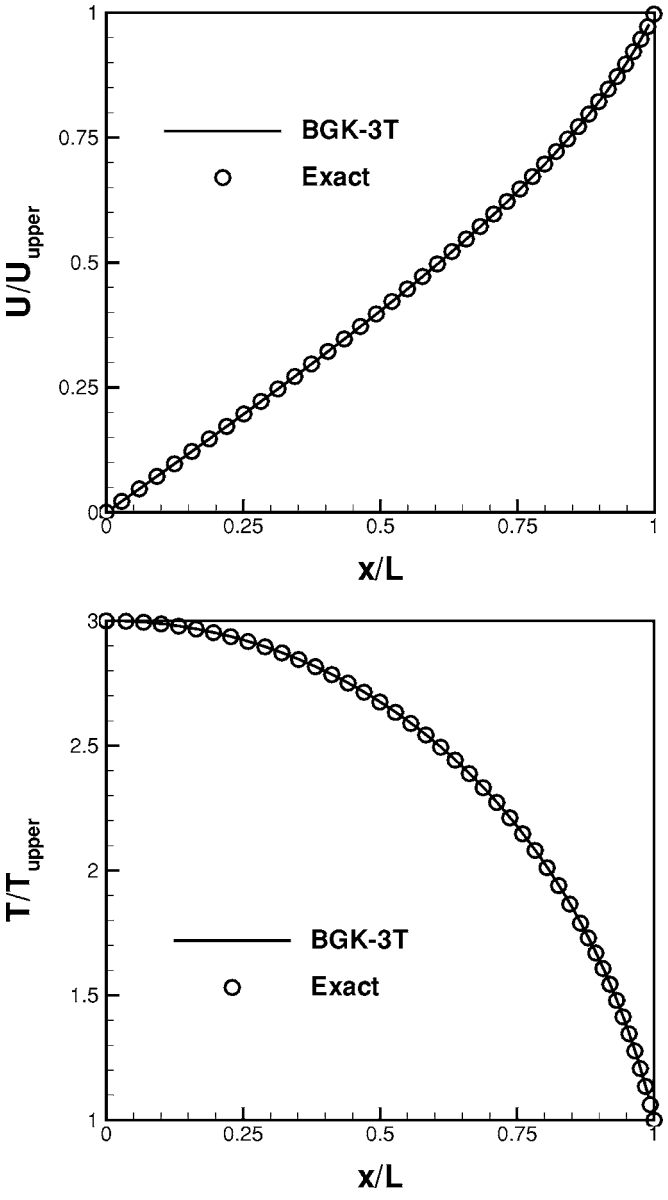

FIG. 2. Velocity U/U_{upper} (top) and temperature T/T_{upper} (bottom) distributions in high-speed Couette flow case for a gas with Pr=2/3, $\mu \sim T$, and Kn=0.001, where the up-plate has a speed of Ma=3.0 and the lower boundary is adiabatic. The circles are analytic Navier-Stokes solutions provided in,[19] and the solid lines are simulation results from the current multiple-temperature model. Multiple temperatures are plotted in the above figure (bottom).

the multi-T model and DSMC results is fair. At this Knudsen number, the velocity profile is not a straight line. The slight curvature near the wall may be due to the Knusden layer in the DSMC solution. In terms of computational efficiency, the multi-T model takes one or two minutes in a PC in all cases to get a steady state solution. Even though we concentrate on the HS molecules in the above simulation, the multi-T model itself can be applied to any molecular model with a generalized viscosity coefficient, such as the Sutherland's law.

B. External force-driven Poiseuille flow

It is generally recognized that in the slip flow regime with Knudsen number $\mathrm{Kn} \leqslant 0.1$, the Navier-Stokes equations

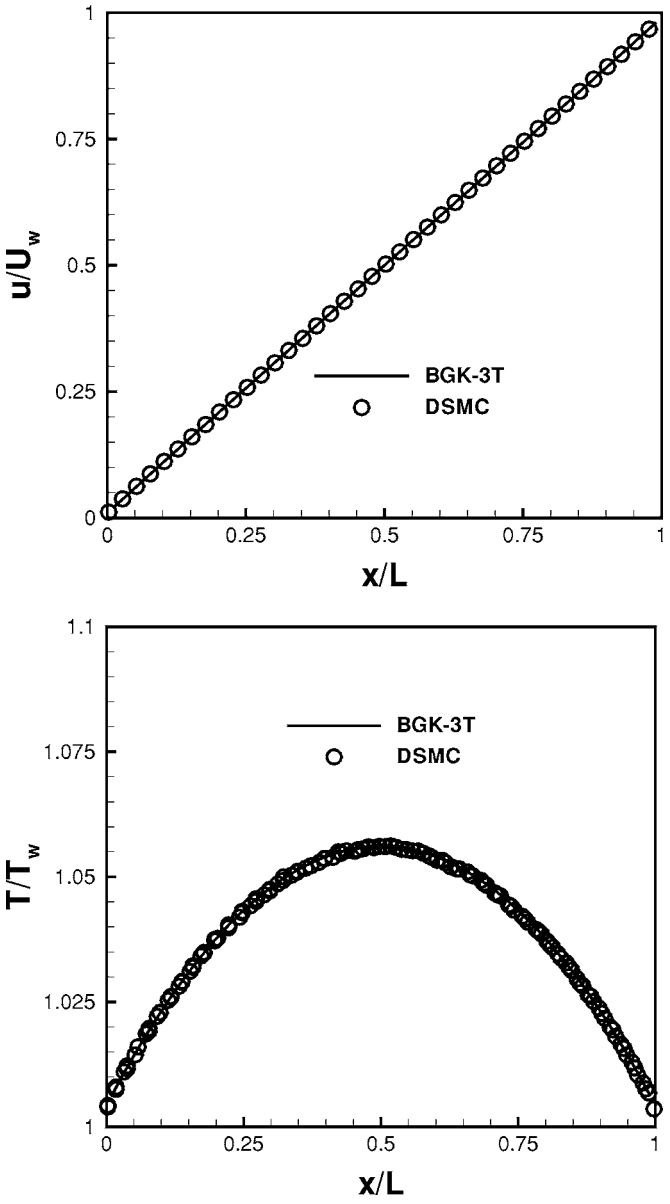

FIG. 3. Velocity U/U_{upper} (top) and temperature T/T_{upper} (bottom) for a gas with Pr=0.68, $\mu \sim \sqrt{T}$, and Kn=0.01, where the up-plate has a speed of U_{upper}=300 m/s. Both boundaries are isothermal with a temperature T=273 K. The circles are DSMC solutions, and the solid lines are simulation results from the current multi-T model.

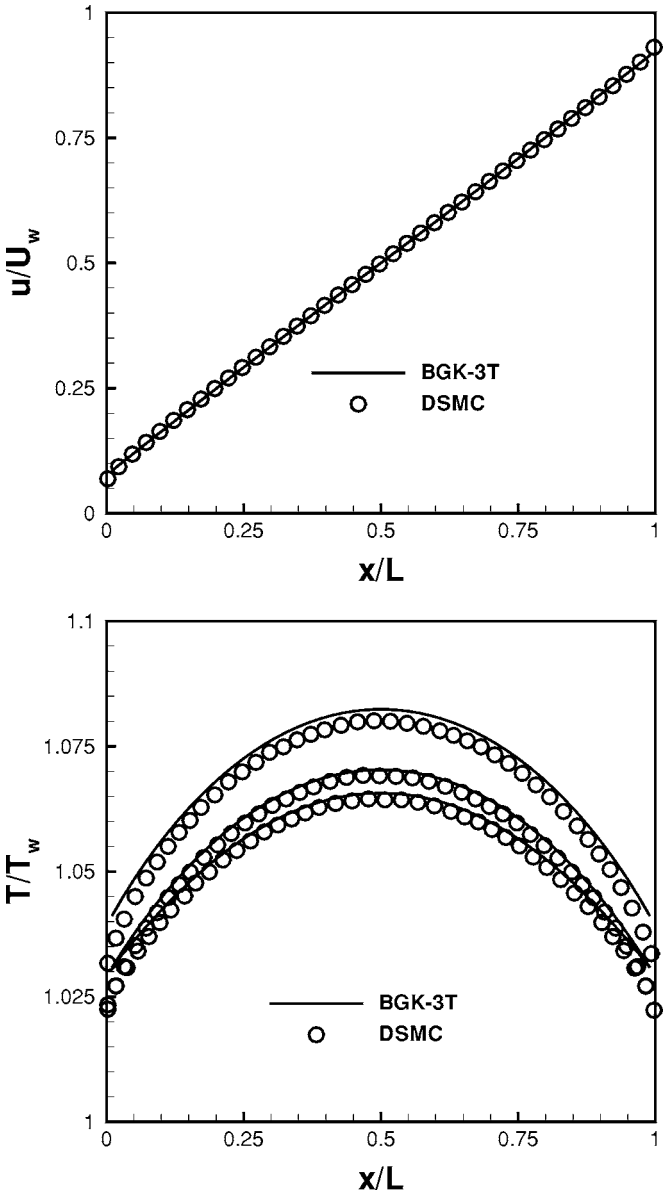

FIG. 4. Velocity U/U_{upper} (top) and temperature T/T_{upper} (bottom) for a gas with Kn=0.1. The circles are DSMC solutions, and the solid lines are simulation results from the current multi-T model. In terms of the temperature distributions, the up one is T_y, the middle one is T_z, and the low one is T_x.

with the slip boundary condition are capable to accurately simulate the microchannel flow. However, for the simple force-driven Poiseuille flow in the slip flow regime with relative small gradient and Knudsen number, the Navier-Stokes equations give qualitatively incorrect predictions.[20,21] For example, they fail to reproduce the central minimum in the temperature profile and nonconstant pressure profile, which are both predicted by the kinetic theory and observed in the DSMC simulations.[22–26] In order to understand these phenomena, many analyses have been done. For example, the nonconstant pressure is well explained based on the Burnett equations,[24] and the temperature minimum at the center is explained only through the kinetic theory,[22,23,26] or the super-Burnett solution.[27] It is interesting to see that the minimal kinetic modeling lattice Boltzmann method can produce the temperature minimum qualitatively as well even though it targets to solve the Navier-Stokes equations.[10]

The setup of external force-driven Poiseuille flow case is given in Ref. 20. The simulation fluid is a hard-sphere gas with particle mass $m=1$ and diameter $d=1$. At the reference density of $\rho_0=1.21\times10^{-3}$, the mean free path is $l_0=m(\sqrt{2}\pi\rho_0 d^2)=186$. The distance between the thermal walls is $L_y=10l_0$ and their temperature is $T_0=1.0$. The reference fluid speed is $U_0=\sqrt{2kT_0/m}=1$, so the Boltzmann constant is taken as $k=1/2$. The reference sound speed is $c_0=\sqrt{\gamma kT_0/m}=0.91$ with $\gamma=5/3$ for a monatomic gas. The reference pressure is $p_0=\rho_0 kT_0/m=6.05\times10^{-4}$. The acceleration is chosen so that the flow will be subsonic and laminar. Specifically, $\rho_0 f=8.31\times10^{-8}$ for the force-driven case. In this case the Knudsen number is $\text{Kn}=l_0/L_y=0.1$ and the

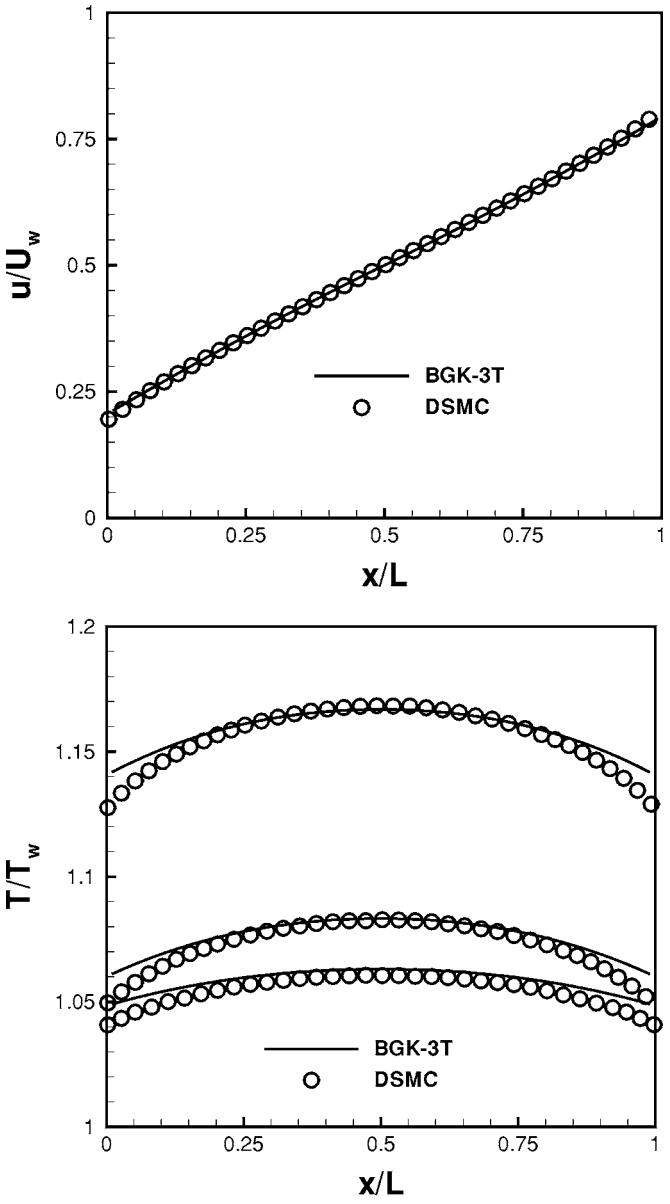

FIG. 5. Velocity U/U_{upper} (top) and temperature T/T_{upper} (bottom) for a gas with Kn=0.5. The circles are DSMC solutions, and the solid lines are results from the current multi-T model. In terms of the temperature distributions, the up one is T_y, the middle one is T_z, and the low one is T_x.

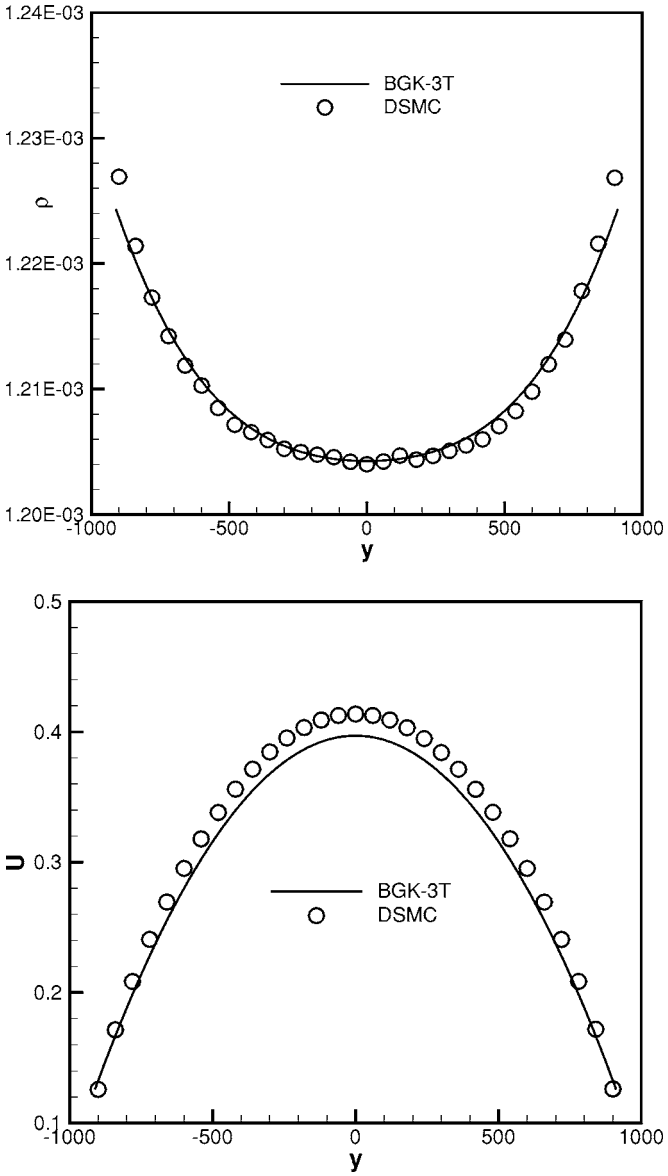

FIG. 6. External force-driven Poiseuille flow at Kn=0.1.[20] Density (top) and velocity (bottom) distributions along the channel cross section, where the circles are DSMC solutions.

Reynolds number is of order 1. In all calculations, the cell side takes the size of one-fifth of the mean free path under the initial flow condition.

Figures 6 and 7 present the results from the current multi-T model. Besides the excellent match of density and velocity between the DSMC and the multi-T results, the curved pressure distribution and temperature are well captured as well. The temperature minimum in both T_x and the averaged temperature T can be clearly observed in Fig. 7. This is surprising because the analysis in[24] confirms that the temperature minimum does not appear even in the Burnett solution. However, it can be recovered in the super-Burnett order.[27] But, based on our current model, even with the inclusion of first-order derivatives in space and time, see Eq. (12), the temperature minimum has been recovered. Thus, the generalized Navier-Stokes equations, where the temperature relaxation term is used to replace the stress and strain relation, have significant physical importance in the capturing of the nonequilibrium thermal effect. In order to distinguish the current solutions from those obtained by solving the standard single-temperature Navier-Stokes equations, the same test case has been calculated by the gas-kinetic BGK-NS method.[17] As shown in Fig. 8, for both pressure and temperature, the BGK-NS method with slip boundary condition for the traditional Navier-Stokes solutions has no the capacity to capture the nonequilibrium thermal effect. This is consistent with the analysis in Ref. 20 and 21.

V. CONCLUSION

In this paper, a gas-kinetic model for the multiple translational temperature is proposed and its corresponding Navier-Stokes equations up to first order of Kn are derived. The difference between the current kinetic model and the

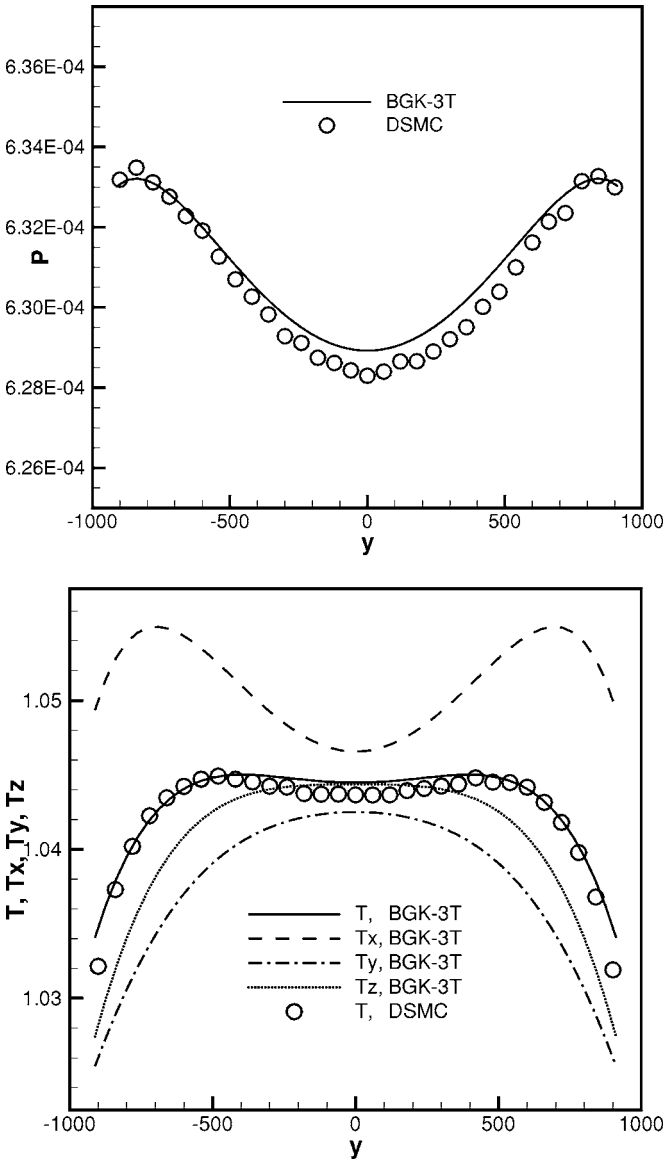

FIG. 7. External force-driven Poiseuille flow at Kn=0.1.[20] Pressure (top) and multiple temperatures (bottom) distributions, where the circles are DSMC solutions. Both the curved pressure and the temperature minimum are recovered from the multi-T model. Solid line (bottom) is the averaged temperature, i.e., $T=(T_x+T_y+T_z)/3$.

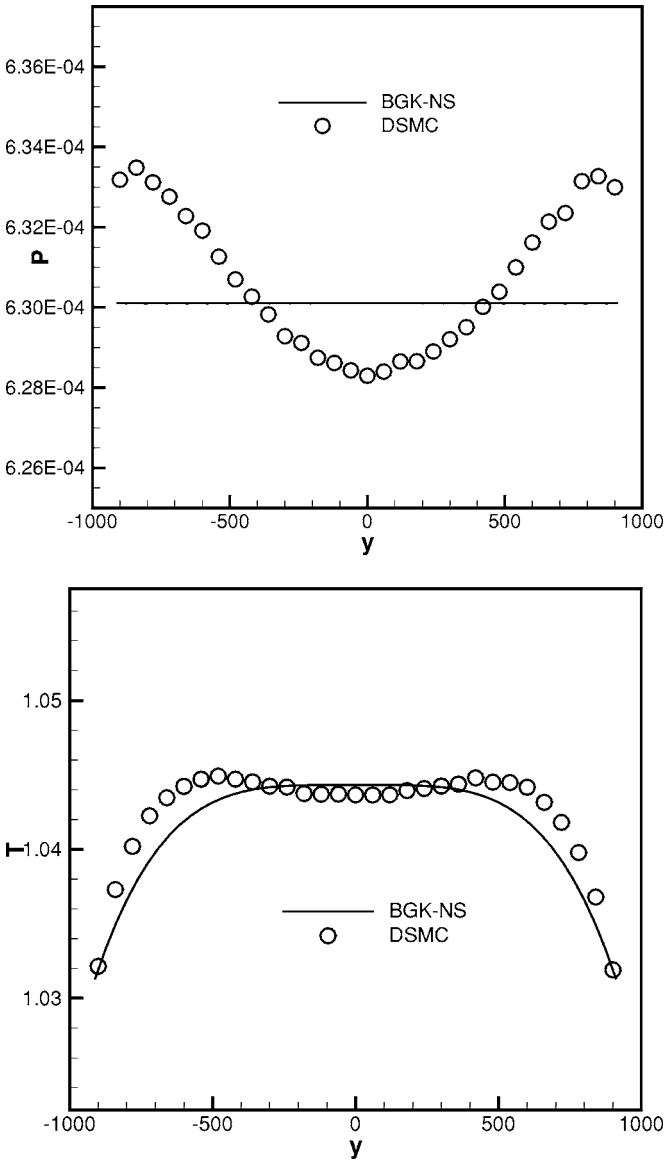

FIG. 8. External force-driven Poiseuille flow at Kn=0.1.[20] Pressure (top) and temperature (bottom) distributions from the BGK-NS method,[17] where the circles are DSMC solutions and the solid lines are the Navier-Stokes solutions. The BGK-NS method basically cannot capture the nonequilibrium effect at Kn=0.1.

ES-BGK mode of Holway is explicitly pointed out. In the generalized Navier-Stokes equations from the current multi-T kinetic model, the assumption between stress and strain in the standard Navier-Stokes equations is replaced by the temperature relaxation term. Based on the numerical examples, it becomes evident that besides modeling slip boundary condition, in the near continuum flow the basic assumption in the Navier-Stokes equations has to be modified. The current model presents such a step to go beyond the Navier-Stokes formulation.

The generalized NS equations are applied to the Couette flow computation in both continuum and near continuum flow regime. As presented theoretically and numerically, this model recovers the Navier-Stokes solutions in the continuum flow regime, such as at the cases $\mathrm{Kn} \leqslant 0.001$. In the transition flow regime, the results from the current model agree well with the DSMC solutions in the capturing of thermal nonequilibrium. Without going up to the Burnett and super-Burnett orders, the nonconstant pressure and the temperature minimum can be well captured by the current extended Navier-Stokes solutions. Therefore, in the slip flow regime, such as Kn=0.1, in order to capture the flow physics the development of multiple-temperature governing equations is important and necessary. The current kinetic model and its numerical method for the extended Navier-Stokes equations provide an alternative effective tool for the study of microflows in the near continuum flow regime, where the DSMC method can be very expensive.

ACKNOWLEDGMENT

This research was supported by Hong Kong Research Grant Council HKUST6102/04E and 621005.

[1] G. E. Karniadakis and A. Beskok, *Microflows: Fundamentals and Simulation* (Springer, New York, 2002).
[2] M. S. Ivanov and S. F. Gimelshein, "Computational hypersonic rarefied flows," Annu. Rev. Fluid Mech. **30**, 469 (1998).
[3] G. Bird, *Molecular Gas Dynamics and the Direct Simulation of Gas Flows* (Clarendon, Oxford, 1994).
[4] Y. Zheng, J. M. Reese, and H. Struchtrup, "Comparing macroscopic continuum models for rarefied gas dynamics: a new test method," J. Comput. Phys. **218**, 748 (2006).
[5] M. J. McNenly, M. A. Gallis, and I. D. Boyd, "Emperical slip and viscosity model performance for microscale gas flow," Int. J. Numer. Methods Fluids **49**, 1169 (2005).
[6] J. Fan and C. Shen, "Statistical simulation of low-speed rarefied gas flows," J. Comput. Phys. **167**, 393 (2001).
[7] Q. Sun and I. D. Boyd, "A direct simulation method for subsonic, microscale gas flows," J. Comput. Phys. **179**, 400 (2002).
[8] F. Toschi and S. Succi, "Lattice Boltzmann method at finite Knudsen numbers," Europhys. Lett. **69**, 549 (2005).
[9] S. Ansumali and I. V. Karlin, "Consistent lattice Boltzmann method," Phys. Rev. Lett. **95**, 260605 (2005).
[10] S. Ansumali," Minimal kinetic modeling of hydrodynamics," Ph.D. thesis, Dissertation No. ETH No 15534, 2004.
[11] K. Xu, "Regularization of the Chapman-Enskog expansion and its description of shock structure," Phys. Fluids **14**, L17 (2002).
[12] K. Xu and E. Josyula, "Continuum formulation for non-equilibrium shock structure calculation," Comput. Phys. Commun. **1**, 425 (2006).
[13] P. L. Bhatnagar, E. P. Gross, and M. Krook, "A model for collision processes in gases. I: Small amplitude processes in charged and neutral one-component systems," Phys. Rev. **94**, 511 (1954).
[14] T. Ohwada and K. Xu, "The kinetic scheme for full Burnett equations," J. Comput. Phys. **201**, 315 (2004).
[15] L. H. Holway, "New statistical models for kinetic theory: methods of construction," Phys. Fluids **9**, 1658 (1966).
[16] E. M. Shakhov, "Generalization of the Krook kinetic equation," Fluid Dyn. **3**, 95 (1968).
[17] K. Xu, "A gas-kinetic BGK scheme for the Navier-Stokes equations and its connection with artificial dissipation and Godunov method," J. Comput. Phys. **171**, 289 (2001).
[18] P. Andries, P. Le Tallec, J. Perlat, and B. Perthame, "The Gaussian-BGK model of Boltzmann equation with small Prandtl numbers," Eur. J. Mech. B/Fluids **19**, 813 (2000).
[19] H. W. Liepmann and A. Roshko, *Elements of Gasdynamics* (Dover, New York, 2001).
[20] Y. Zheng, A. L. Garcia, and B. J. Alder, "Comparison of kinetic theory and hydrodynamics for Poiseuille flow," in *Rarefied Gas Dynamics, 23rd International Symposium*, Whistler, Canada, 20–25 July 2002 (American Institute of Physics, Melville, NY, 2002).
[21] Y. Zheng, A. L. Garcia, and B. J. Alder, "Comparison of kinetic theory and hydrodynamics for Poiseuille flow," J. Stat. Phys. **109**, 495 (2002).
[22] M. Tij and A. Santos, "Perturbation analysis of a stationary nonequilibrium flow generated by an external force," J. Stat. Phys. **76**, 1399 (1994).
[23] M. M. Malek, F. Baras, and A. L. Garcia, "On the validity of hydrodynamics in plane Poiseuille flows," Physica A **240**, 255 (1997).
[24] F. J. Uribe and A. L. Garcia, "Burnett description for plane Poiseuille flow," Phys. Rev. E **60**, 4063 (1999).
[25] S. Hess and M. Malek-Mansour, "Temperature profile of a dilute gas undergoing a plane Poiseuille flow," Physica A **272**, 481 (1999).
[26] K. Aoki, S. Takata, and T. Nakanishi, "Poiseuille-type flow of a rarefied gas between two parallel plates driven by a uniform external force," Phys. Rev. E **65**, 026315 (2002).
[27] K. Xu, "Super-Burnett solutions for Poiseuille flow," Phys. Fluids **15**, 2077 (2003).